



Characterization of the organic matter in sediments of the Great War Island (Belgrade, Serbia)

Sanja Stojadinović¹ · Aleksandra Šajnović¹ · Milica Kašanin-Grubin¹ · Gordana Gajica¹ · Gorica Veselinović¹ · Snežana Štrbac¹ · Branimir Jovančićević²

Received: 29 April 2021 / Accepted: 28 October 2021

© The Author(s), under exclusive licence to Springer-Verlag GmbH Germany, part of Springer Nature 2021

Abstract

Purpose The Great War Island (GWI) is a landform of exceptional features and a protected area located in the center of Belgrade at the Sava and Danube River's confluence. The position of GWI causes a large number of possible hydrocarbons inputs that influence the quality of both river waters and sediments. The main objective of this research is to assess the distribution and source of hydrocarbons in sediments deposited at the GWI depending on the river's flow regimes and depositional environment.

Material and methods Sediment samples were collected from 16 sites (11 sites along the GWI's coast, 4 sites from the inner of the Island, and 1 specific wetland site). The grain size was determined using a standard wet sieving procedure. The extractable organic matter (OM) was quantified after Soxhlet extraction, and aliphatic and aromatic fractions were isolated by column chromatography. *n*-Alkanes, diterpanes, terpanes, steranes, and 16 PAHs are analyzed by gas chromatography-mass spectrometry.

Results and discussion Sand fraction predominates in coastal samples, and clay size fraction in the samples from the inner island environment. The predominance of odd higher *n*-alkanes indicates the terrestrial origin of OM, while the distribution of lower *n*-alkanes indicates a certain proportion of algae, bacteria, and/or high maturity of OM. The presence of oil-type pollutants is confirmed by thermodynamically stable biomarker isomers and/or the presence of unresolved complex mixture (UCM). Inner island samples are characterized by the largest amount of C_{org} (up 6%), indicating high bioproductivity and good preservation of OM. Samples from wetland environment are distinguished by the domination of pimaranes and phyllocladanes among saturated hydrocarbons.

Conclusions This study revealed that sediments of the GWI mainly contain native OM with a certain anthropogenic input. The native OM predominately comes from higher terrestrial plants (*Salix alba*, *Populus nigra*, *Fraxinus viridis*, *Taxodium distichum* Rich.), followed by various types of grasses, macrophytes (*Salvinia natans*, *Nymphaea alba*), bacteria, algae, and phytoplankton. Anthropogenic OM originates from petroleum, but also combustion products arrived by deposition from the air and runoff.

Keywords Alluvial sediments · Organic matter · Aliphatic hydrocarbon · PAH · Great War Island

1 Introduction

Sediments are recognized as excellent sinks for hydrocarbons due to their hydrophobic character and affinity toward particulate matter (Mille et al. 2007). The composition and

distribution of hydrocarbons in sediments are significantly affected by human activities, which is particularly evident in recent decades. Since hydrocarbons can enter the environment by both natural (pyrolysis, diagenesis, biosynthesis, etc.) and anthropogenic processes (industrial activities, combustion of fossil compounds, road traffic, river and sea traffic, oil plants and refineries, oil waste, urban waste, etc.), their origins are multiple, and often challenging to determine. In coastal zones, as a transitional zone between land and river water, the chemical and physical changes can be

Responsible editor: Jan Schwarzbauer

✉ Sanja Stojadinović
sanja.stojadinovic@ihm.bg.ac.rs

Extended author information available on the last page of the article

extreme due to changes in river water levels, strengths of river flow, and possible dry–wet cycles (Tan Pei Jian et al. 2020).

The Great War Island (GWI) is one of the Danube's River islands, and it is located in the central part of Belgrade, Serbia, at the confluence of the Sava and the Danube Rivers. It is a physically exceptional area of Belgrade city with a number of ecological, cultural, historical, and recreational values as well as by the richness of the living world. Bearing in mind the position and characteristics of the GWI (Kašanin-Grubin et al. 2019) and consequently large number of possible hydrocarbon inputs, it is of great interest to study in detail their origin.

The application of organic geochemical investigations tool is useful for the determination of hydrocarbon sources in sediments (Peters et al. 2005; Jovančičević et al. 2007). A pool of aliphatic diagnostic indices and more particular signatures can be used to identify biogenic or anthropogenic sources. The distribution of polycyclic aromatic hydrocarbon (PAH) is also useful to differentiate the hydrocarbons main sources, particularly to distinguish petrogenic from pyrogenic hydrocarbons (Yunker et al. 2002; and reference in; Soclo et al. 2000; Scheibye et al. 2014).

The Great War Island is under the direct influence of the urban environment as the main source of pollution. This paper represents the first extensive study of the sources and spatial distribution of aliphatic hydrocarbons and PAHs in

the coastal sediments of Great War Island, as well as in the flooded inner part of the island. The main objective of this research is to assess the distribution of hydrocarbons in sediments depending on the flow regimes of Sava and Danube Rivers, respectively depositional environment, and to find out the source of aliphatic hydrocarbons and PAHs using biomarkers and PAH compositions.

2 Materials and methods

2.1 Study area

The Great War Island area is located between 1172 and 1169 km of the Danube River and it consists of two river islands, the Great War Island and Small War Island (SWI). The island is positioned at 500 m of the airline from the city center of Belgrade, Serbia and directly lies on the international waterways of the rivers Danube and Sava (Fig. 1).

The GWI is a sedimentary, alluvial-accumulative formation and one of its most essential characteristics is the constant change of its shape and size. This is a consequence of the continual process of slowing and accelerating transportation and accumulation of sediments. On average, the GWI covers a total area of ~196 ha and an average elevation of the Island is 72 m above sea level

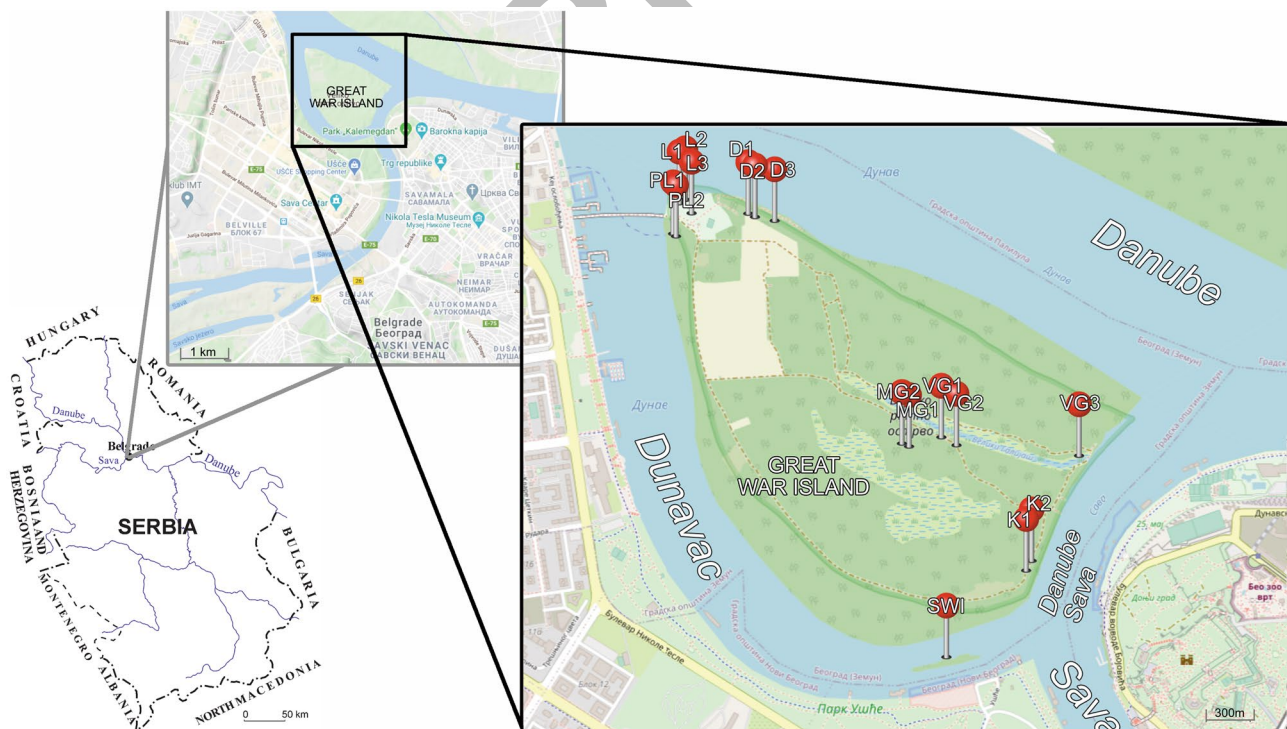


Fig. 1 Location of the Great War Island (GWI), Belgrade, and sampling locations of the GWI: Danube (D), Kalemegdan (K), Lido (L), Veliki Galijaš (VG), Mali Galijaš (MG), Small War Island (SWI), Port Lido (PL)

(a.s.l.). The average sediment thickness is estimated at 25 m.

The geographical area is plain, from 69.5 m a.s.l. in the center of the Island to 73.5 m a.s.l. on the upstream part of the Island, the surrounding of Lido beach (Fig. 1). Therefore, an entire surface of the Island is inclined toward the Danube stream, i.e., toward the east. The mild unevenness in the field is the result of an irregular accumulation of sediments during the floods.

The whole GWI contains sensitive and complex ecosystems and preserved areas important for species and communities that inhabit it and play a major role in maintaining the biodiversity of the wider coastal area and the city itself. Some species of migrating wetland birds, considered an international treasure, use this habitat for nesting, feeding or resting during North–South migrations. Position and biodiversity of the island give the island the special protection status, and in April 2005 GWI was placed under protection as an area of importance for the protection of the environment and cultural and historical heritage in accordance with corresponding regulations and laws of the Republic of Serbia (Off. Gazette No. 7 2005).

2.2 Sampling

Sampling sites were chosen in order to best represent the influence of the Sava and Danube Rivers on the GWI and therefore samples were collected from coastal and inner parts of Islands (Table 1; Fig. 1). A sampling of sediments was conducted during October 2019. Surface sediment samples (~ 700 g) were collected with a small shovel, placed in

glass jars, and transported to the laboratory. At the North, the Great War Island is surrounded by the Danube River (samples D1–D3, L1–L3), on the east by the Sava (K1, K2), and on the south and west by the Danube channel—Dunavac (PL1, PL2, SWI). The SWI site is a specific wetland environment and most of the time it is under the water. The channels Veliki Galijaš and Mali Galijaš are located in the inner part of the Island, and they are under the indirect influence of the flow of the two rivers (VG1–VG3, MG1, and MG2). Sediments in these channels are deposited only at the time when the whole Island is flooded.

2.3 Methods

Collected samples were cleaned from plant and shell residues and air-dried at room temperature for a week. The dried samples were gently pounded, and subsequently the reduction of the sample size was done by quartering.

Grain size analysis was performed according to a standard wet sieving procedure using the following sieve sizes: 1, 0.5, 0.25, 0.125, and 0.063 mm. The sieved material was dried in an oven and weighed. The size fraction < 0.063 mm was analyzed using the standard pipette method. Getting the percentages of each fraction allowed dividing sediments into three principal categories: sand, silt and clay.

The content of organic carbon (C_{org}) was determined by elemental analysis. The dry samples were pre-treated with diluted hydrochloric acid (1:3, v:v) to eliminate carbonates. The elemental analyses were conducted using a Vario EL III, CHNOS Elemental Analyzer (Elementar Analysen-system GmbH). The extractable organic matter (bitumen) in the samples was obtained by Soxhlet's method with an azeotropic

Table 1 List of samples with results of grain size analysis and group organic-geochemical parameters

Location	Sample	Grain size			Bitumen (ppm in sediment)	Hydrocarbons (% in bitumen)
		Sand (%)	Silt (%)	Clay (%)		
Danube	D1	31.72	53.27	15.01	587	31.3
	D2	90.00	8.02	1.98	137	33.2
	D3	94.00	3.94	2.06	148	12.2
Lido	L1	23.94	57.44	18.62	790	24.1
	L2	89.29	10.00	0.71	257	15.6
	L3	99.88	0.12	0.00	52	33.5
Port Lido	PL1	98.81	1.19	0.00	135	35.3
	PL2	56.14	40.00	3.86	872	6.9
Veliki Galijaš	VG1	32.5	48.31	19.19	1660	13.9
	VG2	47.27	40.31	12.42	2670	15.7
	VG3	42.34	48.51	9.15	1069	7.5
Mali Galijaš	MG1	31.47	48.25	20.28	1340	22.4
	MG2	31.53	50.94	17.54	870	6.9
Across from Kalemegdan	K1	77.07	19.12	3.81	970	23.7
	K2	33.71	46.86	19.43	1050	10.5
Small War Island	SWI	9.74	71.17	19.06	1434	27.3

mixture of methylene chloride and methanol (36 h) and quantified. The content of extractable organic matter in the samples was determined from the ratio of the extract mass (dried to constant mass) and the initial mass of the sample. Bitumen was separated into three fractions by column chromatography (diameter of the column: 1 cm). The saturated hydrocarbons were eluted using 25 ml *n*-hexane, the aromatics using 38.5 ml benzene, while the NSO fraction was eluted using a 50 ml mixture of chloroform and methanol (1:1, v/v) from 10 mg of bitumen. As sorbent, 2.25 g SiO₂ and 1.65 g Al₂O₃ were used previously activated at 180 °C for 12 h. The saturated and aromatic hydrocarbons fractions were analyzed by gas chromatography-mass spectrometry (GC-MS). The instrument used was Agilent Technologies 7890A gas chromatograph coupled to an Agilent 5975C mass selective detector (operated at an electron energy of 70 eV). Samples were injected in split mode (1:5) onto HP5-MS capillary column (30 m in length, 0.25 mm id, film thickness 0.25 μm). The injection volume was 1 μl. Helium 5.0 (99.999 %) was the carrier gas with a constant flow rate of 1.5 ml/min. The following operating temperatures were used: injector—250 °C, interface (transfer line)—280 °C, ion source—230 °C, quadrupole—150 °C, while the temperature of column was programmed from 80 to 310 °C at a rate of 2 °C/min and the final temperature of 310 °C was maintained for an additional 25 min. GC-MS analysis was performed in the scan mode from *m/z* 45 to *m/z* 600. Detailed analyses of the target compounds were conducted using ion chromatograms given in Table 2. The individual peaks were identified by comparison with literature data (Peters et al. 2005; Wang et al. 2016) and based on their mass spectra, library: NIST11. Biomarker and aromatics parameters were calculated from GC-MS chromatogram peak areas (ChemStation Enhanced Data Analysis Software, Agilent Technologies).

2.4 Organic-geochemical indexes

Based on the distribution and abundance of *n*-alkanes, several indices were calculated to identify the hydrocarbon sources (natural vs. anthropogenic) found in the investigated samples:

Table 2 Characteristic fragment ions for characterization of compounds by GCMS

<i>m/z</i>	Compounds	<i>m/z</i>	Compounds
71	<i>n</i> -alkanes	178	phenanthrene and anthracene
123	diterpanes	202	fluoranthene and pyrene
191	terpanes	228	benzo[a]anthracene and chrysene
217	steranes	234	retene
128	naphthalene	252	benzo[b]fluoranthene and benzo[k]fluoranthene
152	acenaphthylene	252	benzo[a]fluoranthene and perylene
154	acenaphthene	276	indeno[1,2,3-c,d]pyrene and benzo[g,h,i]perylene
166	fluorene	278	dibenzo[a,h]anthracene

- Carbon Preference Index (CPI) represents the relative abundance of odd over even carbon chain lengths and was calculated for the full range of *n*-alkanes as:

$$\text{CPI}(C_{14} - C_{33}) = \frac{1}{2} * [(\Sigma_{\text{odd}}(n - C_{15} - n - C_{31}) / \Sigma_{\text{even}}(n - C_{14} - n - C_{30}) + \Sigma_{\text{odd}}(n - C_{15} - n - C_{31}) / \Sigma_{\text{even}}(n - C_{16} - n - C_{32}))] \quad (1)$$

An *n*-alkane distribution with a strong predominance of odd long-chain homologues show that terrestrial organic matter contributed to the precursor biomass. On the other hand, an elevated concentration of lower homologues indicates algal organic matter input and/or high maturity. In petroleum, *n*-alkanes have uniform distribution of odd and even homologues (CPI is about 1) (Peters et al. 2005).

In this paper, in addition to the CPI values for the entire range of *n*-alkanes, the ratios of odd and even *n*-alkane homologues for lower *n*-alkanes (CPI₁) and mid- and long-chain *n*-alkanes (CPI₂) calculated by the following formulas:

$$\text{CPI}_1(C_{14} - C_{22}) = \frac{1}{2} * [(\Sigma_{\text{odd}}(n - C_{15} - n - C_{21}) / \Sigma_{\text{even}}(n - C_{14} - n - C_{20}) + \Sigma_{\text{odd}}(n - C_{15} - n - C_{21}) / \Sigma_{\text{even}}(n - C_{16} - n - C_{22}))] \quad (2)$$

$$\text{CPI}_2(C_{23} - C_{33}) = \frac{1}{2} * [(\Sigma_{\text{odd}}(n - C_{25} - n - C_{31}) / \Sigma_{\text{even}}(n - C_{24} - n - C_{30}) + \Sigma_{\text{odd}}(n - C_{25} - n - C_{31}) / \Sigma_{\text{even}}(n - C_{26} - n - C_{32}))] \quad (3)$$

- Terrestrial to Aquatic Ratio (TAR) can be used for determination of land or marine based *n*-alkanes. It is calculated following Bourbonniere and Meyers (1996):

$$\text{TAR} = \frac{(n - C_{27} + n - C_{29} + n - C_{31})}{(n - C_{15} + n - C_{17} + n - C_{19})} \quad (4)$$

The odd predominance in higher *n*-alkanes indicates the terrestrial origin of organic matter (TAR > 1), while the distribution of lower *n*-alkanes indicates a certain proportion of algae, bacteria, and/or high maturity of organic matter (TAR < 1).

- Short/long-chain *n*-alkanes ($n\text{-C}_{17} + n\text{-C}_{19} + n\text{-C}_{21}$)/($n\text{-C}_{27} + n\text{-C}_{29} + n\text{-C}_{31}$) and $n\text{-C}_{17}/n\text{-C}_{27}$ ratios were calculated to determine the dominant bacteria, algae or phytoplankton-derived and/or higher plant-derived organic matter.
- Proxy ratio (P_{aq}) was defined by Ficken et al. (2000) as:

$$P_{aq} = (n\text{-C}_{23} + n\text{-C}_{25}) / (n\text{-C}_{23} + n\text{-C}_{25} + n\text{-C}_{29} + n\text{-C}_{31}) \quad (5)$$

This parameter reflects the submerged/floating aquatic macrophyte input to organic matter relative to that from the terrestrial plants. Odd numbered mid-chain *n*-alkanes including *n*-C₂₃ and *n*-C₂₅ are abundant in submerged and emerged vegetation.

- Average chain length (ACL₂₇₋₃₃) is the weighted average of the various carbon chain lengths, depending upon the types of vegetation, latitude, and climatic condition, while petrogenic inputs decrease the values of ACL. ACL is defined as:

$$ACL_{27-33} = \frac{(27 \times n\text{-C}_{27} + 29 \times n\text{-C}_{29} + 31 \times n\text{-C}_{31} + 33 \times n\text{-C}_{33})}{(n\text{-C}_{27} + n\text{-C}_{29} + n\text{-C}_{31} + n\text{-C}_{33})} \quad (6)$$

- Ratios $n\text{-C}_{27}/n\text{-C}_{31}$ and $n\text{-C}_{29}/n\text{-C}_{31}$ were used in order to determine contribution of woody plants and grass. Both grass and trees produce *n*-C₂₇, *n*-C₂₉, and *n*-C₃₁, but usually *n*-C₃₁ is most abundant in grass while *n*-C₂₇ or *n*-C₂₉ is most abundant in trees (Li et al. 2016).
- Natural *n*-alkanes ratio (NAR) is calculated using equation (Mille et al. 2007):

$$NAR = \frac{[\Sigma n\text{-alk}(C_{19} - C_{32}) - 2 \Sigma \text{even } n\text{-alk}(C_{20} - C_{32})]}{(\Sigma n\text{-alk}(C_{19} - C_{32}))} \quad (7)$$

The values of the natural *n*-alkane ratio (NAR) are between 0.18 and 0.61. This ratio roughly estimates the proportions of natural and petroleum *n*-alkanes. Values of NAR are close to zero for petroleum hydrocarbons and close to one for higher terrestrial plants (Mille et al. 2007).

2.5 PAH ratios

PAH diagnostic ratios have been designed and used to distinguish the sources of PAHs due to their stability, physical and chemical attributes (Yunker et al. 2002 and reference in; Budzinski et al. 1997; Baumard et al. 1998; Soclo et al. 2000; Scheibye et al. 2014; Witt and Trost, 1999). Several indices were calculated:

- Ratio of low-molecular-weight—LMW (2–3 rings), and high-molecular-weight—HMW (4–6 rings) compounds

abundances (LMW/HMW). This ratio is very useful to distinguish between petrogenic (> 1 values) and pyrolytic (< 1 values) origin of PAH (Soclo et al. 2000);

- Anthracene/(Anthracene plus Phenanthrene) ratio—(Phe/(Phe + Ant)) values of this ratio indicate a petrogenic origin when values are below 0.10 while values > 0.10 are characteristic of combustion-derived PAHs. (Phe/(Phe + Ant)) ratio is often plotted against the Fluoranthene/(Fluoranthene plus Pyrene) ratio (Fluo/(Fluo + Pyr)) (Budzinski et al. 1997);
- Fluoranthene/(Fluoranthene plus Pyrene)—(Fluo/(Fluo + Pyr)) values of this ratio < 0.40 indicate uncombusted petroleum, values between 0.40 and 0.50 indicate liquid fossil fuel combustion, and ratios > 0.50 indicate grass, wood, or coal combustion;
- Benz[a]anthracene/(Benz[a]anthracene plus Chrysene)—(BaA/(BaA + Chr)); Yunker et al. 2002 estimates that ratio values of this ratio < 0.20 indicate petroleum, values between 0.20 and 0.35 either petroleum or combustion

sources, and values > 0.35 indicate combustion (Yunker et al. 2002);

- Indeno[1,2,3-cd]pyrene/(Indeno[1,2,3-cd]pyrene plus Benzo[ghi]perylene)—(IdP/(IdP + BPer)) values of this ratio < 0.20 indicate petroleum, values between 0.20 and 0.50 indicate mixed petroleum and combustion PAH's origin, while values of this ratio > 0.50 is indication of grass, wood, and coal combustion.

3 Results

3.1 Grain size analysis

Grain size of the GWI sediments varies with the flow energy and the place of deposition on the Island. Sediments deposited in the inner Island parts (VG, MG) have similar composition and are poorly sorted sandy clayey silts. These sediments are deposited only during major floods when the whole Island is under water. Coastal sediments vary from well sorted sands to silts, with varying portions of sand fractions. This composition is a reflection of the energy of the flow of both Sava and Danube rivers. Sands are mostly deposited in the NW edge of the Island in sediments brought by the Danube. Silt component is higher in sediments deposited at the confluence of Sava and Danube (K), and Danube channel (PL1, PL2, SWI) (Table 1, Fig. 2).

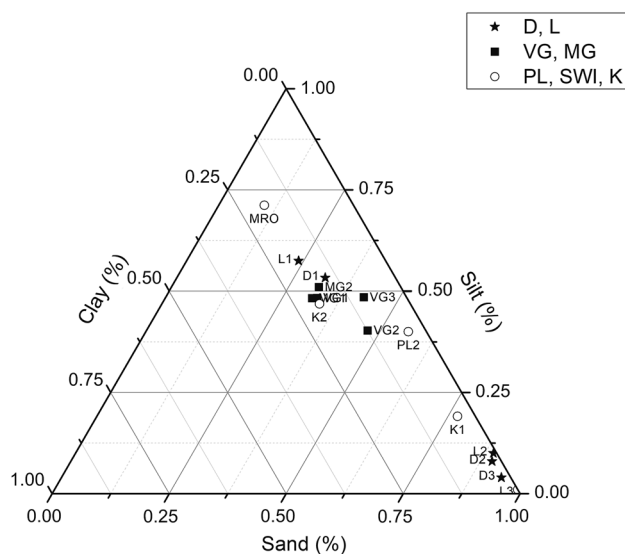


Fig. 2 Grain-size distribution of sediments from the Great War Island. (D—Danube, L—Lido, VG—Veliki Galijaš, MG—Mali Galijaš, PL—Port Lido, SWI—Small War Island, K—Kalemegdan)

3.2 Aliphatic hydrocarbon's composition—general overview

The range of the extractable organic matter's quantities, bitumen, in the sediment is 52–2670 ppm with an average value of 865 ppm (Table 1). The highest values (> 1000 ppm) are found in sites VG1–VG3 (inner part of the GWI). These sites are characterized by the high values of C_{org} (4.01–6.06). The lowest values of bitumen (< 300 ppm) are characterized sand sediments (% sand > 90, Table 1). A relatively small contribution of hydrocarbons in the bitumen varies significantly (6.9–35.3%) (Table 1).

Based on the appearance of the total ion current (TIC) chromatograms of the saturated fractions (Fig. 3), it is noticeable *n*-alkanes are the most dominant components in almost all samples. The only exception is a sample at the site—SWI, which is, as mentioned above, specific since it is under water most of the time. The total ion current of the samples D1–D3 and L1–L3 which are on the influence of the main Danube River stream (Fig. 1) is characterized by *n*-alkanes followed by pimarane and phyllocladane, as well as the presence of hopanes (Fig. 3). The other specific characteristic of these TICs is a hump in the total ion chromatogram. That hump is known as unresolved complex mixture (UCM). Expressive domination of diterpenes, pimarane, and phyllocladane in saturated fraction, followed by *n*-alkanes is characterized for the SWI site.

The remarkably similar distribution of *n*-alkanes and hopanes in TIC, followed by UCM, is observed in samples of locations Port Lido (PL1, PL2), Kalemegdan (K1, K2),

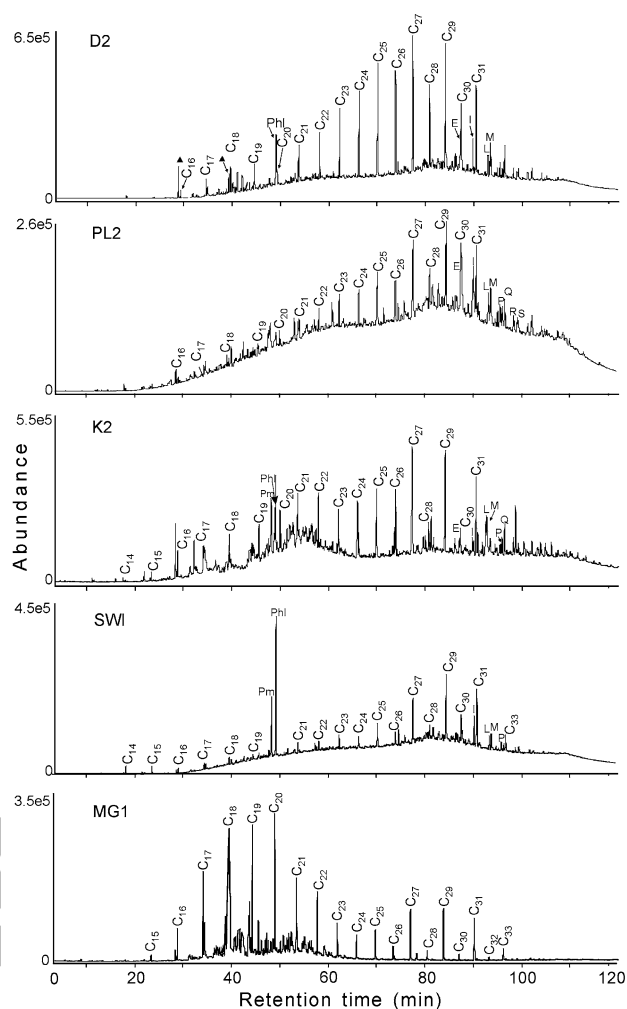


Fig. 3 Total ion current (TIC) of selected samples. Pm—Pimarane; Phl—16(α)H-Phyllocladane; black triangle—*n*-alkane; for abbreviations E–S, see legend of Fig. 5. Danube (D), Kalemegdan (K), Mali Galijaš (MG), Small War Island (SWI), Port Lido (PL)

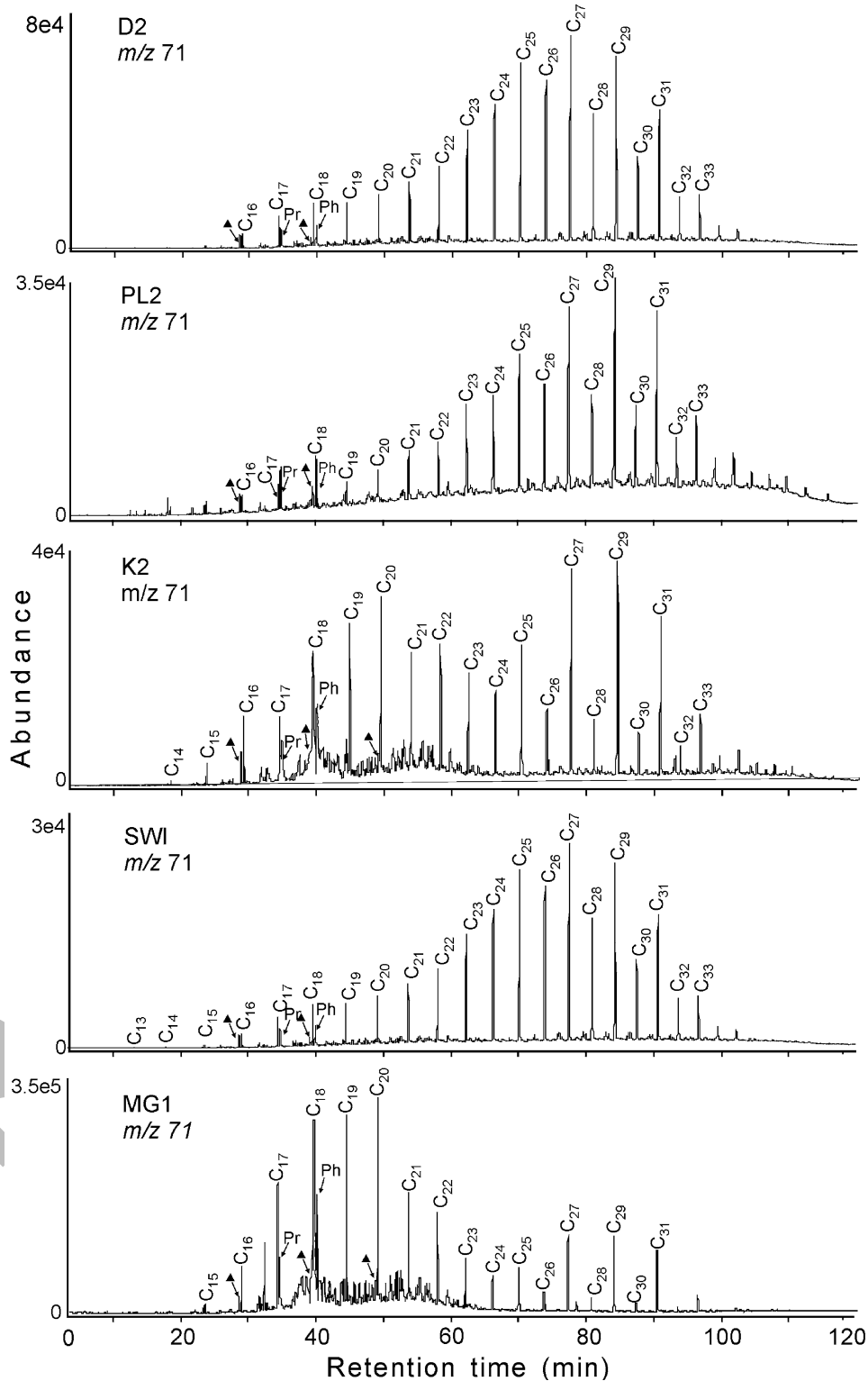
and Veliki Galijaš enter (VG3), but hopanes are not so pronounced (Fig. 3).

On the other side, saturated hydrocarbons of the inner Island samples (MG1, MG2, VG1, and VG2) differ significantly from coastal samples. They are characterized by the domination of *n*-alkanes and terpanes, pimarane and phyllocladane, as well as the absence of UCM and hopanes (Fig. 3).

3.3 *n*-Alkanes and isoprenoids

The *n*-alkanes were identified based on a fragment of ion m/z 71 (Fig. 4), and it is the dominant group of compounds in almost all samples. Generally, the *n*-alkane shows a bimodal distribution with Carbon number maxima (C_{max}) at C_{20} or C_{19} and at C_{27} or C_{29} (Table 3). The exception is the MG1

Fig. 4 Fragmentograms of m/z 71 n -alkanes and isoprenoids. (*Pr* pristane; *Ph* phytane; black triangle n -alkenes). Danube (D), Kalemegdan (K), Mali Galijaš (MG), Small War Island (SWI), Port Lido (PL)



sample, where lower n -alkanes are dominant, with n -C₂₀ maximum (Fig. 4).

The n -alkane patterns in range C₂₃–C₃₅ were characterized by a marked odd over even predominance, with a maximum at n -C₂₇ or n -C₂₉, which resulted in high CPI

values for full distribution of n -alkanes (C₁₄–C₃₃) and high CPI₂ values (exception sample MG1, Table 3). The lower n -alkanes, C₁₄–C₂₂, showed a uniform distribution of odd and even homologs (CPI₁, Table 3; Fig. 4). This distribution of n -alkanes is also reflected on the values of the

Table 3 Values of parameters calculated from distributions and abundances of *n*-alkanes and isoprenoids

Sample	<i>n</i> -alkane range	C_{max}	CPI	CPI ₁	CPI ₂	Pr/Ph	$n-C_{17}/n-C_{27}$	$n-C_{27}/n-C_{31}$	$(n-C_{17}+n-C_{19}+n-C_{21})/(n-C_{27}+n-C_{29}+n-C_{31})$	TAR	Paq	ACL	NAR
D1	C ₁₆ –C ₃₃	C ₂₉	1.71	1.25	3.86	0.72	0.11	1.16	0.22	10.14	0.31	29.19	0.35
D2	C ₁₆ –C ₃₅	C ₂₇	1.25	1.05	2.52	0.97	0.10	1.58	0.20	9.92	0.44	29.07	0.18
D3	C ₁₇ –C ₃₃	C ₂₇	1.31	1.55	2.62	0.49	0.04	1.88	0.12	18.71	0.44	28.93	0.18
L1	C ₁₆ –C ₃₄	C ₂₉	1.39	1.55	2.76	0.78	0.59	0.84	0.34	3.74	0.35	29.68	0.23
L2	C ₁₆ –C ₃₃	C ₂₇ , C ₂₉	1.55	1.16	3.49	0.85	0.20	1.68	0.22	7.06	0.38	29.01	0.29
L3	C ₁₆ –C ₃₁	C ₂₇	1.31	0.98	3.48	0.63	0.28	1.35	0.60	3.11	0.48	28.81	0.22
PL1	C ₁₆ –C ₃₃	C ₂₇	1.87	1.13	5.11	0.72	0.13	1.43	0.28	7.09	0.35	29.14	0.39
PL2	C ₁₆ –C ₃₄	C ₂₉	1.53	1.27	3.24	0.78	0.08	1.19	0.14	17.92	0.34	29.31	0.30
VG1	C ₁₅ –C ₃₃	C ₂₇	2.69	1.38	8.80	0.77	0.05	2.43	0.21	9.73	0.29	28.71	0.51
VG2	C ₁₄ –C ₃₃	C ₂₇	2.64	1.45	8.67	0.80	0.20	4.98	0.22	4.17	0.41	28.31	0.54
VG3	C ₁₅ –C ₃₃	C ₂₉	1.39	0.97	3.04	0.72	0.13	0.95	0.18	9.66	0.32	29.41	0.23
MG1	C ₁₅ –C ₃₁	C ₂₀	0.87	0.64	7.82	0.37	1.53	1.06	1.89	0.75	0.40	28.96	0.24
MG2	C ₁₆ –C ₃₃	C ₂₉	3.30	1.12	8.92	0.46	0.04	1.34	0.07	31.98	0.24	29.05	0.61
K1	C ₁₆ –C ₃₃	C ₂₉	1.68	1.36	5.32	0.78	0.39	1.39	0.77	2.17	0.37	29.18	0.27
K2	C ₁₄ –C ₃₃	C ₂₉	1.83	1.28	6.38	0.82	0.31	1.38	0.56	2.91	0.36	29.16	0.34
SWI	C ₁₃ –C ₃₃	C ₂₉	2.31	1.26	5.97	1.03	0.13	0.78	0.21	9.08	0.22	29.52	0.49

CPI carbon preference index; Pr pristane; Ph phytane; $CPI(C_{14}-C_{33}) \frac{1}{2} * [(\sum \text{odd}(n-C_{15}-n-C_{31}) / \sum \text{even}(n-C_{14}-n-C_{30}) + \sum \text{odd}(n-C_{15}-n-C_{31}) / \sum \text{even}(n-C_{16}-n-C_{32}))]$; $CPI_1(C_{14}-C_{22}) \frac{1}{2} * [(\sum \text{odd}(n-C_{15}-n-C_{21}) / \sum \text{even}(n-C_{14}-n-C_{20}) + \sum \text{odd}(n-C_{15}-n-C_{21}) / \sum \text{even}(n-C_{16}-n-C_{22}))]$; $CPI_2(C_{23}-C_{33}) \frac{1}{2} * [(\sum \text{odd}(n-C_{21}-n-C_{31}) / \sum \text{even}(n-C_{20}-n-C_{30}) + \sum \text{odd}(n-C_{21}-n-C_{31}) / \sum \text{even}(n-C_{22}-n-C_{32}))]$; $TAR (n-C_{27} + n-C_{29} + n-C_{31}) / (n-C_{15} + n-C_{17} + n-C_{19})$; $Paq (n-C_{23} + n-C_{25}) / (n-C_{23} + n-C_{25} + n-C_{29} + n-C_{31})$; $ACL_{27-33} (27 \times n-C_{27} + 29 \times n-C_{29} + 31 \times n-C_{31} + 33 \times n-C_{33}) / (n-C_{27} + n-C_{29} + n-C_{31} + n-C_{33})$; $NAR [\sum n\text{-alk}(C_{19}-C_{32}) - 2 \sum \text{even } n\text{-alk}(C_{20}-C_{32})] / (\sum n\text{-alk}(C_{19}-C_{32}))$

parameters TAR, $n-C_{17}/n-C_{27}$, and $(n-C_{17} + n-C_{19} + n-C_{21}) / (n-C_{27} + n-C_{29} + n-C_{31})$ (Table 3). The values of the natural *n*-alkane ratio (NAR) are between 0.18 and 0.61. This ratio roughly estimates the proportions of natural and petroleum *n*-alkanes, and values of NAR are close to zero for petroleum hydrocarbons and close to one for higher terrestrial plants (Mille et al. 2007). Phyllocladane and pimarane are dominant among saturated hydrocarbons in samples from the SWI wetland environment (Table 1, Figs. 1 and 3).

The isoprenoids pristane (Pr) and phytane (Ph) are present in most samples. The values of Pr/Ph ratio in investigated samples between 0.37 and 1.03 (Table 3) indicate that organic matter of majority sediments was deposited under slightly reducing conditions (Peters et al. 2005).

3.4 Terpanes and steranes

Terpane and sterane biomarkers were identified on the base of *m/z* 191 and *m/z* 217 fragmentogram, respectively. The typical distributions of steranes and terpanes are shown in Fig. 5. Terpanes are present in all investigated sediments samples, while steranes are absent in Mali Galijaš samples (MG1, MG2). The peaks of thermodynamically stable isomers C₃₀ 17 α (H)21 β (H)-hopane, and C₂₉ 17 α (H)21 β (H)-hopane are the most dominant in

m/z 191 chromatograms of all samples, as well as typical geo-isomers, 18 α (H)-neohopanes. C₃₁–C₃₅ homohopanes are also present as a pair of C₂₂ diastereoisomers (22S, 22R). Homohopanes 22(S) isomers are more abundant than less stable 22(R) form. Values of the ratio Ts/(Ts + Tm) involving 18 α (H)-22,29,30-trisnorhopane (Ts) and 17 α (H)-22,29,30-trisnorhopane (Tm) are between 0.36 and 0.45 (Table 4). As mentioned above, steranes and diasteranes are present in almost all analyzed samples. In steranes configuration, besides isomers of regular sterane configurations 14 α (H)17 α (H)20(R), isomers with a thermodynamically stable configuration of 14 α (H)17 α (H)20(S), 14 β (H)17 β (H)20(R), and 14 β (H)17 β (H)20(S), as well as typical geo isomers 13 β (H)17 α (H) and 13 α (H)17 β (H) were also identified. The values of specific organic-geochemical parameters calculated from the distributions of steranes biomarkers are given in Table 4.

The sterane type biomarkers, characteristic for petroleum and its derivatives, have only not been identified, or are present in low abundance, in samples taken from the central part of the Great War Island (channel Mali Galijaš, Sample MG1 and MG2, Fig. 1). Samples from the central part of the island, from channel Veliki Galijaš (VG1 and VG2) are under the constant influence of river water, and oil pollutants from the river can reach this site by the river water.

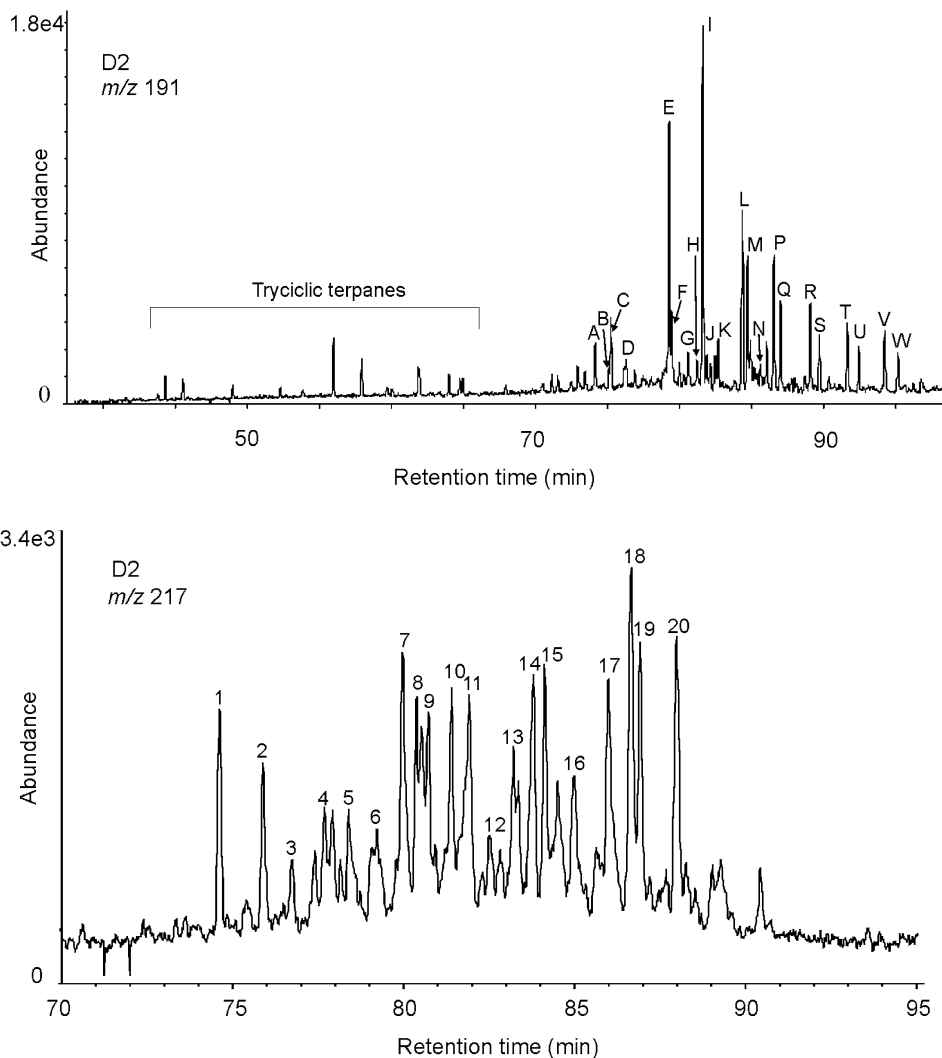


Fig. 5 Typical GC–MS terpanes and C_{27} – C_{29} steranes and diasteranes distribution. A—Ts ($C_{27}18\alpha(H)$ 25,29,30 trisnorhopane); B— C_{27} -hop5(6)-ene; C—Tm ($C_{27}17\alpha(H)$ 25,29,30 trisnorhopane); D— $C_{27}17\beta(H)21\beta(H)$ -hopane; E— $C_{29}17\alpha(H)21\beta(H)$ -hopane; F— C_{29} Ts; G— $C_{29}17\beta(H)21\alpha(H)$ -moretane; H—Oleanane; I— $C_{30}17\alpha(H)21\beta(H)$ -hopane; J— C_{30} -hop17(21)-ene; K— $C_{30}17\beta(H)21\alpha(H)$ -moretane; L— $C_{31}17\alpha(H)21\beta(H)22(S)$ hopane; M— $C_{31}17\alpha(H)21\beta(H)22(R)$ hopane; N—Gammacerane; P— $C_{32}17\alpha(H)21\beta(H)22(S)$ -hopane; Q— $C_{32}17\alpha(H)21\beta(H)22(R)$ -hopane; R— $C_{33}17\alpha(H)21\beta(H)22(S)$ -hopane; S— $C_{33}17\alpha(H)21\beta(H)22(R)$ -hopane; T— $C_{34}17\alpha(H)21\beta(H)22(S)$ -hopane; U— $C_{34}17\alpha(H)21\beta(H)22(R)$ -hopane; V— $C_{35}17\alpha(H)21\beta(H)22(S)$ -hopane; W— $C_{35}17\alpha(H)21\beta(H)22(R)$ -hopane; 1— $C_{27}13\beta(H)17\alpha(H)20(S)$ -diasterane; 2— $C_{27}13\beta(H)17\alpha(H)20(R)$ -diasterane; 3— $C_{27}13\alpha(H)17\beta(H)20(S)$ -diasterane;

4— $C_{27}13\alpha(H)17\beta(H)20(R)$ -diasterane; 5— $C_{28}13\beta(H)17\alpha(H)20(S)24(S+R)$ -diasterane; 6— $C_{28}13\beta(H)17\alpha(H)20(R)24(S+R)$ -diasterane; 7— $C_{28}13\alpha(H)17\beta(H)20(S)$ -diasterane + $C_{27}14\alpha(H)17\alpha(H)20(S)$ -sterane; 8— $C_{29}13\beta(H)17\alpha(H)20(S)$ -diasterane + $C_{27}14\beta(H)17\beta(H)20(R)$ -sterane; 9— $C_{28}13\alpha(H)17\beta(H)20(R)$ -diasterane + $C_{27}14\beta(H)17\beta(H)20(S)$ -sterane; 10— $C_{27}14\alpha(H)17\alpha(H)20(R)$ -sterane; 11— $C_{29}13\beta(H)17\alpha(H)20(R)$ -diasterane; 12— $C_{29}13\alpha(H)17\beta(H)20(S)$ -diasterane; 13— $C_{28}14\alpha(H)17\alpha(H)20(S)$ -sterane; 14— $C_{29}13\alpha(H)17\beta(H)20(R)$ -diasterane + $C_{28}14\beta(H)17\beta(H)20(R)$ -sterane; 15— $C_{28}14\beta(H)17\beta(H)20(S)$ -sterane; 16— $C_{28}14\alpha(H)17\alpha(H)20(R)$ -sterane; 17— $C_{29}14\alpha(H)17\alpha(H)20(S)$ -sterane; 18— $C_{29}14\beta(H)17\beta(H)20(R)$ -sterane; 19— $C_{29}14\beta(H)17\beta(H)20(S)$ -sterane; 20— $C_{29}14\alpha(H)17\alpha(H)20(R)$ -sterane

3.5 Aromatic hydrocarbons

The analysis of aromatic compounds can also determine possible specific sources of hydrocarbons in the investigated sediments. Among the aromatic compounds, natural polyaromatic hydrocarbons (PAHs), as well as polyaromatic hydrocarbons of anthropogenic origin, were found

(Fig. 6). Perylene and retene, natural aromatic compounds, were found in almost all analyzed samples (except for VG samples, and MG1 which are presented in traces). The most likely precursors of biogenic five-ringed PAH, perylene could be types of black pigments found in modern plants, insects, crinoids, and fungi or have a diatomaceous origin (Tan and Heit 1981; Varnosfaderany et al. 2014), since

Table 4 Values of parameters calculated from distributions and abundances of terpanes and steranes

Sample	$C_{31}\alpha\beta S / (C_{31}\alpha\beta S + C_{31}\alpha\beta R)$	Ts/(Ts + Tm)	$C_{29}\alpha\alpha S / (C_{29}\alpha\alpha R + C_{29}\alpha\alpha S)$	$C_{29}\beta\beta S / (C_{29}\beta\beta S + C_{29}\beta\beta R)$	$C_{27} \text{ dia} / (C_{27} \text{ dia} + C_{27}\alpha\alpha R)$
D1	0.58	0.40	0.55	0.56	0.37
D2	0.57	0.44	0.54	0.55	0.44
D3	0.57	0.38	0.49	0.57	0.37
L1	0.63	0.48	0.61	0.59	0.37
L2	0.55	0.38	0.46	0.57	0.42
L3	0.55	0.39	0.47	0.50	0.46
PL1	0.57	0.39	0.54	0.58	0.41
PL2	0.56	0.36	0.45	0.47	0.44
VG1	0.61	0.38	0.56	0.60	0.37
VG2	0.59	n.d	0.55	0.60	0.38
VG3	0.56	0.38	0.47	0.53	0.31
MG1	trace	trace	n.d	n.d	n.d
MG2	0.62	0.44	n.d	n.d	n.d
K1	0.56	0.40	0.45	0.54	0.30
K2	0.60	0.43	0.57	0.54	0.38
SWI	0.56	0.50	0.56	0.54	0.40

$C_{31} \alpha\beta S$ $C_{31}17\alpha(H)21\beta(H)22(S)$ hopane; $C_{31} \alpha\beta R$ $C_{31}17\alpha(H)21\beta(H)22(R)$ hopane; Ts $C_{27}18\alpha(H) 25,29,30$ trisnorhopane; Tm $C_{27}17\alpha(H) 25,29,30$ trisnorhopane; $C_{29}\alpha\alpha S$ $C_{29} 14\alpha(H)17\alpha(H)20(S)$ -sterane; $C_{29}\alpha\alpha R$ $C_{29} 14\alpha(H)17\alpha(H)20(R)$ -sterane; $C_{29}\beta\beta R$ $C_{29} 14\beta(H)17\beta(H)20(R)$ -sterane; $C_{29}\beta\beta S$ $C_{29} 14\beta(H)17\beta(H)20(S)$ -sterane; $C_{27}\alpha\alpha R$ $C_{27} 14\alpha(H)17\alpha(H)20(R)$ -sterane; $C_{27} \text{ dia}$ $C_{27} 13\beta(H)17\alpha(H)20(R)$ -diasterane; *n.d.* not determined

coniferous wood and higher plants are sources of retene (Ramdahl 1983). Sources of the PAH contamination in sediments (pyrolytic or petrogenic) have been investigated by studying the general fingerprint and by using several PAH diagnostic ratios (Yunker et al. 2002). Several PAH ratios

are presented in Table 5. The first step in discrimination of petrogenic and pyrolytic contamination is comparing low molecular weight (LMW) and high molecular weight (HMW) compound abundances (Witt and Trost 1999; Scheibye et al. 2014). LMW/HMW ratio at all analyzed

Fig. 6 Typical GCMS chromatogram of PAHs for sample PL2. *m/z* 152 (acenaphthylene), *m/z* 154 (acenaphthene), *m/z* 166 (fluorene, Flu), *m/z* 178 (phenanthrene, Phe and anthracene, Ant), *m/z* 202 (fluoranthene, Fluo and pyrene, Py), *m/z* 228 (benzo[a]anthracene, B[a]A and chrysene, Chr), *m/z* 234 (retene), *m/z* 252 (benzo[b]fluoranthene, B[b]Fluo; benzo[k]fluoranthene, B[k]Fluo; benzo[a]fluoranthene, B[a]Fluo; perylene), *m/z* 276 (indeno[1,2,3-c,d]pyrene and benzo[g,h,i]perylene) and *m/z* 278 (dibenzo[a,h]anthracene, DB[a,h]A)

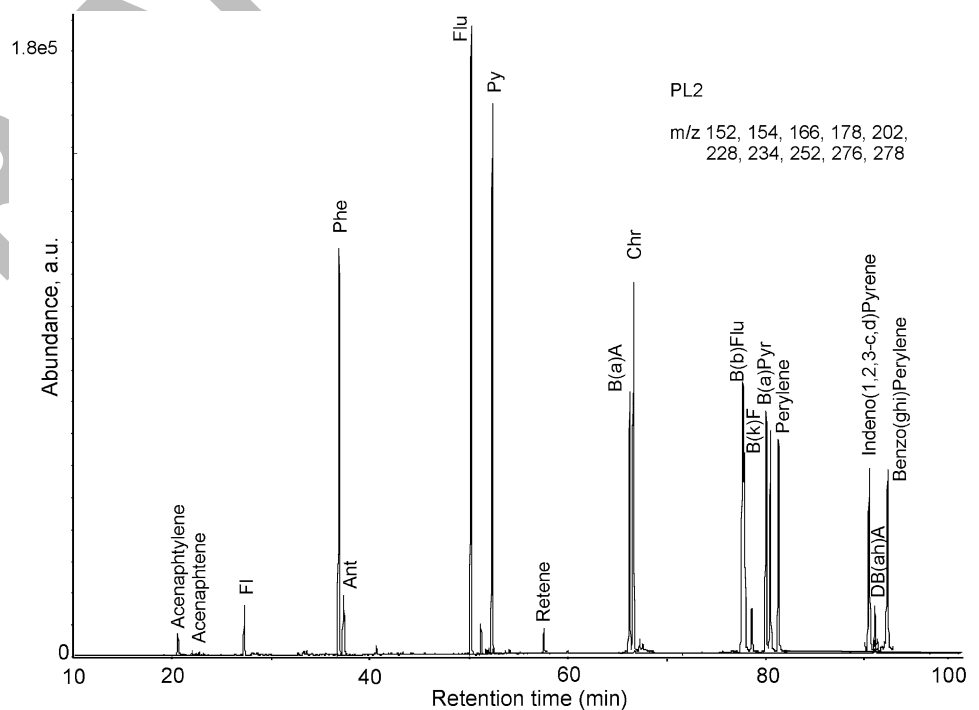


Table 5 Values of PAH diagnostic ratios

Sample	LMW/HMW	MPs/P	Fluo/ (Fluo + Pyr)	Ant/(Ant + Phe)	IP/(IP + Bghi)	BaP/BghiP	BaA/ (BaA + Chr)
D1	0.07	0.88	0.54	0.06	0.52	1.08	0.20
D2	0.14	0.60	0.56	0.08	0.54	1.19	0.33
D3	0.17	0.65	0.56	0.04	0.60	1.53	0.33
L1	0.06	0.98	0.54	0.07	0.55	1.23	0.23
L2	0.17	0.69	0.55	0.06	0.55	1.24	0.35
L3	0.20	0.72	0.55	0.02	0.57	1.34	0.37
PL1	0.12	0.74	0.53	0.07	0.58	1.36	0.32
PL2	0.15	0.54	0.54	0.14	0.54	1.16	0.40
VG1	0.08	0.98	0.59	0.23	0.72	2.62	0.18
VG2	0.19	0.63	0.68	0.28	0.55	1.24	0.27
VG3	0.12	0.88	0.52	0.05	0.58	1.36	0.16
MG1	0.51	0.43	0.60	0.00	0.68	2.13	0.12
MG2	0.08	0.82	0.55	0.00	0.48	0.91	0.34
K1	0.11	0.61	0.56	0.00	0.54	1.18	0.32
K2	0.07	0.69	0.57	0.04	0.53	1.14	0.44
SWI	0.07	0.38	0.55	0.06	0.56	1.29	0.27

LMW low molecular weight polyaromatic hydrocarbons, HMW high molecular weight polyaromatic hydrocarbons, MP methylphenanthrene, P phenanthrene, Fluo fluoranthene, Ant Anthracene, Pyr pyrene, IP Indeno(123 cd)piren, BaA benzo[a]anthracene, Chr chrysene, BaP benzo[a]pyrene, BghiP benzo[ghi]perylene

samples was lower than one (ranged between 0.07 and 0.43, Table 5). Values of calculated diagnostic ratios, Ant/(Ant + Phe), BaA/(BaA + Chr) and IdP/(IdP + BPer) are plotted against Fluo/(Fluo + Ant) in Fig. 7.

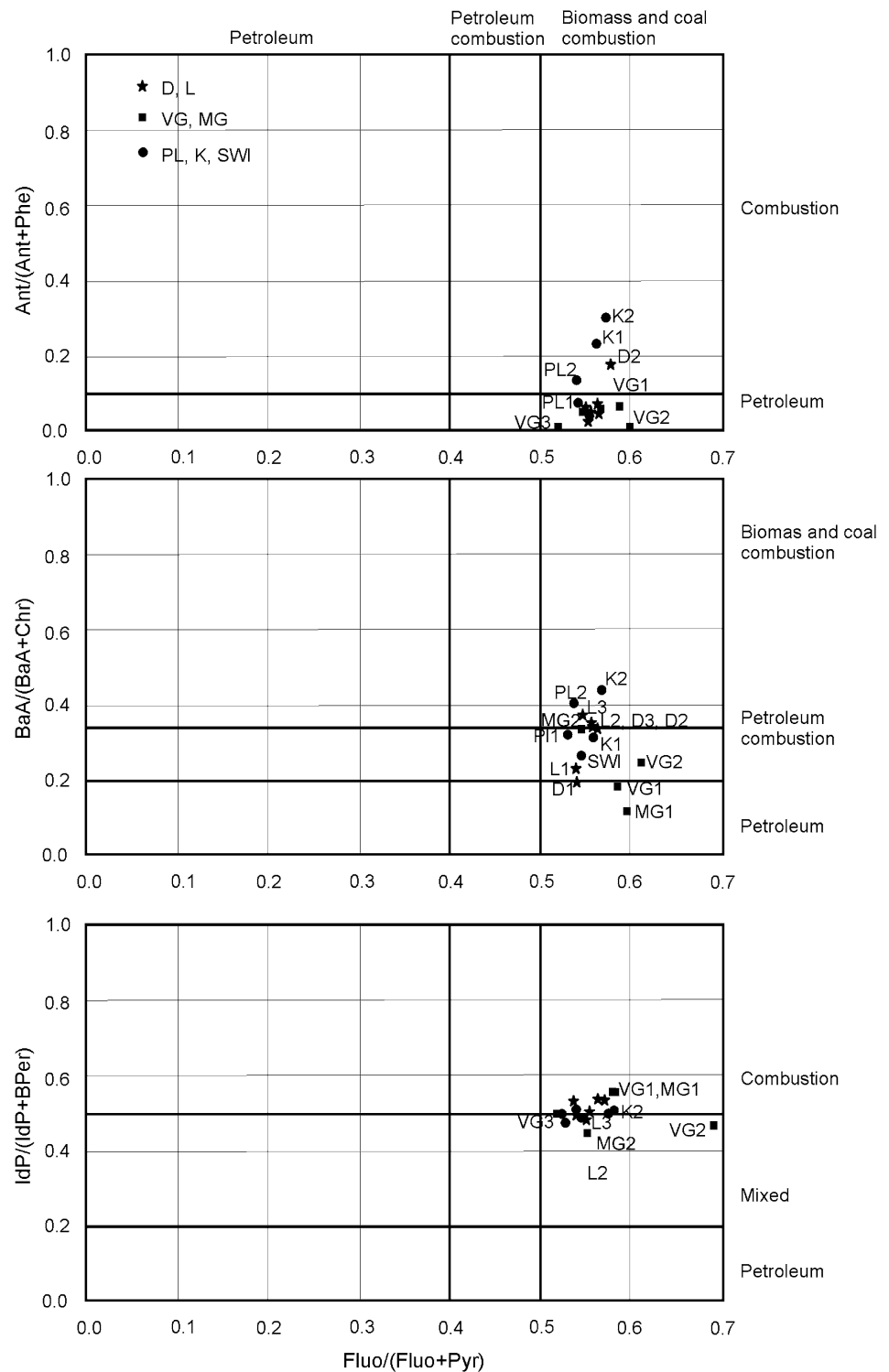
4 Discussion

4.1 Main stream of Danube

The composition of coastal sediments D1–D3 and partly of L1–L3 is a consequence of the high energy main Danube river flow that transports them (Fig. 1). Sediments D1–D3 contain a relatively low amount of extractable organic matter with a significant contribution of saturated and aromatic hydrocarbons (Table 1). The saturated hydrocarbon fraction of samples D1–D3 (Fig. 2) is dominated by higher odd *n*-alkanes and thermodynamically stable hopanes isomers. This distribution is unusual since higher odd alkanes indicate a native organic matter, and thermodynamically stable hopanes an anthropogenic source. Other members of the homologous series such as alkanes, especially lower alkanes, are present in subordinate amount. The lower even *n*-alkanes (*n*-C₁₆ and *n*-C₁₈) are followed by corresponding *n*-alkenes (Fig. 4). Generally, alkenes have a biogenic origin, and the presence of *n*-alkenes is an indicator of the contribution of the native organic matter (Volkman et al. 1998; Mille et al. 2007; Aloulou et al. 2010; Stojadinović et al. 2021). It is known that light-molecular weight *n*-alkanes are

more bioavailable for microbial degradation than heavy ones (Yang et al. 2021). Bearing in mind these facts, it can be assumed that the phenomenon of biodegradation of the oil pollutant occurs even before it reaches the investigated location (D1–D3). This indicates that conditions were favorable for biodegradation of oil pollutants, primarily regarding temperature, presence of nutrients especially nitrogen, phosphorus, and in some cases iron, and aerobic conditions (Das and Chandran, 2011), which can all be linked with the fast river flow and better water mixing. The distribution of *n*-alkanes with a maximum at *n*-C₂₇ or *n*-C₂₉ along with the predominance of odd homologues imply that these surface sediments contain native organic matter of terrestrial origin (*Fraxinus viridis*, *Salix alba*, *Taxodium distichum* Rich, *Salvinia natans*, *Nymphaea alba*). In addition to this, in the saturated fraction of samples D1–D3, the presence of diterpanes pimarane and phyllocladane, which are also known as indicators of wetland plants, is significant. The presence of phyllocladane and pimarane in investigated sediments is in agreement with the widespread existence of conifers, *Taxodiaceae* on GWI (Off Gazette No. 50/93, 93/93, 10/94, 1994). Based on the distribution of terpanes and steranes in the saturated fractions of the sediments and the values of the corresponding maturity parameters (Table 4), it could be confirmed that investigated sediments, in addition to native organic matter, contain organic matter of anthropogenic origin. Furthermore, almost identical distributions of these biomarkers in D1–D3 samples represent evidence of the same petroleum pollutants' presence (Table 4, Fig. 5).

Fig. 7 PAH isomer pair ratios of sediments. (D—Danube, L—Lido, VG—Veliki Galijaš, MG—Mali Galijaš, PL—Port Lido, SWI—Small War Island, K—Kalemegdan)



Sediments from the site Lido (L1–L3, Fig. 1) are characterized by the predominance of odd higher n -alkanes in the distribution of saturated hydrocarbons. Compared with samples D1–D3, low chain n -alkanes are more abundant, which is reflected through TAR parameter (Table 3). Values of maturity parameters calculated based on sterane and

hopanes distribution are in good agreement with values of these parameters in petroleum (Mackenzie 1984; Peters et al. 2005; Štrbac et al. 2014; Samelak et al. 2018, 2020), indicating that anthropogenic organic matter is the same as in the samples D1–D3 (Table 4, Fig. 5).

4.2 Slow flow of the Danube channel and confluence

The sites Port Lido (PL) and SWI are under the effect of the slower flow in the Danube channel—Dunavac (Fig. 1), which is shallower and narrower, than the main flow (Fig. 1). This is particularly evident at the SWI site, where the low flow energy combined with high deposition rates leads to the formation of a wetland environment (Table 1, Fig. 1). The sites Kalemegdan (K1, K2) and Veliki Galijaš—enter (VG-3) are particularly interesting since they are at the confluence, thus under the influence of both Sava and Danube Rivers.

The samples from sites Port Lido and Kalemegdan are characterized by the dominance of *n*-alkanes and the presence of unresolved complex mixture (UCM) as well as the trace of hopanes in the total ion chromatogram (Fig. 3). Therefore, petroleum input and/or a biodegraded petroleum pollutant is occurring in these samples (Frysiner et al. 2003; Wang et al. 2011; Silva et al. 2012). Compared to samples from main stream of Danube, hopanes in TIC of Port Lido and Kalemegdan are not so distinct.

The aliphatic fraction of Kalemegdan samples and VG3 sample is characterized by a particularly pronounced bimodal distribution of *n*-alkanes, and there are two conspicuous (expressed) maxima in these samples (*n*-C₂₀ and *n*-C₂₆). Typically, the abundance of C₂₇, C₂₉, and C₃₁ with odd-carbon number predominance is an indicator of terrestrial plants, whereas the dominance of the *n*-alkanes in the range C₁₈–C₂₄ with uniform odd and even distribution of *n*-alkanes can suggest oil input (Fig. 4) (Wang et al. 2011). The native organic matter originates from higher land plants characteristic of the lower parts of the island, such as *Salix alba*, *Salix amygdalina*, *Populus nigra*, *Fraxinus viridis*, *Taxodium distichum Rich* (Off Gazette No. 50/93, 93/93, 10/94, 1994), as well as from various grass species, emergent and submerged macrophytes such as *Salvinia natans*, *Nymphaea alba* (Off Gazette No. 50/93, 93/93, 10/94, 1994), as well as from bacteria, algae, and phytoplankton. The presence of phyllocladane and pimarane (Fig. 3) also confirms the partially terrestrial origin of organic matter, which is in accordance with an abundance of conifers on the island (Off Gazette No. 50/93, 93/93, 10/94, 1994).

In Port Lido's samples, higher odd alkanes are the most dominant, highlighting the significant contribution of terrestrial origin's organic matter, which has already been pointed out.

The saturated hydrocarbons in the SWI sample are dominated by diterpanes pimarane and 16 α (H)phyllocladane, which are known as indicators of conifers (Otto and Wilde 2001), with a lower or higher proportion of *n*-alkanes with a predominance of higher odd homologues (Figs. 3 and 4). This distribution suggests significant conifer *Taxodiaceae*

contribution to organic matter to the SWI sample (Otto and Wilde 2001). The obtained result is in agreement with an abundance of *Taxodium distichum Rich* on this island (Šijačić-Nikolić et al. 2010; Off Gazette No. 50/93, 93/93, 10/94, 1994). This distribution, together with low sand content in these sediments, is typical for a calm shallow sedimentation environment (swamp) and indicates a native organic matter with mostly terrestrial plants as precursors.

Samples from the SWI based on the distribution of *n*-alkanes and *n*-alkanes parameters differ significantly from the GWI's samples (Fig. 4, Table 3). Furthermore, they have a remarkably lower contribution of algae, bacteria, fungi, reeds, floating macrophytes, i.e., the SWI's samples are dominated by more terrestrial plants as a precursor of organic matter. The low proxy value of *n*-alkanes of aqueous macrophytes, Paq (Table 3), emphasizes this statement.

4.3 Inner part of the island

The two longitudinal depressions (channels) called the Veliki Galijaš and Mali Galijaš are located in the inner part of the Island, and they are under the indirect influence of the flow of the two rivers. Sediments in these channels are deposited at the time when the whole Island is flooded (Fig. 1), which happens once or twice a year (Kašanin-Grubin et al. 2019). In October 2007, the rehabilitation of the Veliki Galijaš channel was completed, as well as cleaning, draining, and bringing it back to its previous functional condition. The samples from this part contain the largest amount of C_{org} (up to 6%), indicating possible high bioproductivity and good preservation of the organic matter (Peters et al. 2005; Schwarzbauer and Jovančičević 2015). In addition, they contain a relatively low amount of saturated and aromatic hydrocarbons (Table 1). These values may be an indicator of the low degree of maturation of the organic matter, as well as unpolluted to moderately polluted sediments (Peters et al. 2005; Štrbac et al. 2014; Samelak et al. 2018). They are deposited under the most pronounced reduction conditions (parameter Pr/Ph, Table 3) in comparison with other investigated sediments. Pronounced reduction conditions are a good precondition for the preservation of organic matter. Group and specific organic-geochemical parameters indicate that most of the examined samples frequently contain native organic matter with subordinate anthropogenic organic matter. Hydrocarbons that are characteristic of oil and its derivatives are not present even at the trace level in the samples from Mali Galijaš, which can be explained by the fact that to this part of the GWI sediment is brought only during major floods. It is noticeable that the mentioned samples have a characteristic bimodal distribution (Fig. 4). Most samples are dominated by higher *n*-alkanes, except MG1 sample, where lower *n*-alkanes are dominant, coinciding with the TAR parameter's value, further indicating the mixed origin

of the organic matter (Fig. 3, Table 3). This distribution of saturated hydrocarbons indicates the presence of a native organic matter that originates mainly from higher terrestrial plants. The values of the NAR parameter (Table 3) confirm the predominant native organic matter in the VG and MG2 samples in contrast to the coastal sediments. Higher odd n -C₂₇ and n -C₂₉ alkanes predominate, as the evidence for terrestrial precursor biomass, i.e., woody plants' presence, is in agreement with the significant presence of diterpanes (Fig. 3). It is known that there are 11 species of trees on the Island, five of which are autochthonous. The *Salix alba* L. represents a dominant species of regularly flooded alluvial *Salicetum albae* communities (Off Gazette No. 50/93, 93/93, 10/94., 1994). In addition, mid-chain n -alkanes (n -C₂₅) are also abundant, indicating the presence of marsh plants, which are building entire "underwater meadows" in the central part of the island. These plants are on the list of plant species protected as natural rarities: *Ceratophyllum demersum*, *Myriophyllum spicatum*, *Spirodela polyrrhiza*, *Salvinia natans*, and *Nymphaea alba* (Off. Gazette No. 50/93, 93/93, 10/94. 1994).

4.4 Anthropogenic organic matter

Anthropogenic organic matter of the petroleum type is present in 14 of investigated samples of GWI's sediments. The distribution of biomarkers was characterized by a predominance of the thermodynamically more stable isomers (Fig. 4). Namely, geoisomers can be present only in mature organic matter—ancient sediments or oil. Since native mature organic matter cannot be present in recent river sediment, certain anthropogenic input of organic matter in investigated sediments is indicated (Peters et al. 2005). Furthermore, almost identical distributions of these biomarkers and similar values of corresponding maturity parameters (Table 4) in all samples represent evidence that the sediments of the GWI contain petroleum pollutants from the same source. In addition, some samples contain unresolved complex mixture (UCM) as a possible indicator of the petroleum input (Volkman et al. 1992). In the central part of the Great War Island (channels Mali Galijaš and Veliki Galijaš), characteristic petroleum biomarkers and their derivatives have not only been identified at all, or they are present in low amounts.

Diagnostic PAH parameters and plots Ant/(Phe + Ant) = f(Fluo/(Fluo + Pyr)), BaA/(BaA + Chr) = f(Fluo/(Fluo + Pyr)), and IdP/(IdP + BPer) = f(Fluo/(Fluo + Pyr)) (Fig. 7) were used to distinguish anthropogenic organic matter sources. LMW/HMW ratio at all analyzed samples was lower than one (Table 5), suggesting the predominance of pyrolytic origin. Domination of pyrogenic PAHs in GWI's samples implies that the incomplete combustion of organic matter is a dominant source of PAHs. Based on PAH ratios shown in

Fig. 7, it is assumed that in sites D1–D3 and L1–L3 anthropogenic organic matter originated from petroleum or combustion of coal or petroleum. There is no significant difference in PAH distribution between the samples of this group and the samples from the coast which are in contact with fast river flow (samples D1–D3, L1–L3) (Fig. 7). Similar results were obtained for samples which were taken from the slow flow of the Danube channel and confluence and inner part of the Island. The PAH ratios indicate a possible mixed combustion source, e.g., from petroleum, grass, wood, and/or coal combustion (Fig. 7). Bearing in mind the inner part of the Island is under protected regime, the presence of anthropogenic PAH compounds especially in the MG samples is probably the consequence of the permanently atmospheric deposition and runoff from urban areas over decades. Finally, it can be concluded that a primary source of PAHs in all investigated samples of GWI are combustion processes and that it reaches sediments by atmospheric deposition and runoff.

5 Conclusions

The sediments of the Great War Island, a natural protected area in the center of Belgrade city, were investigated with the main objective to explore the influence of different flow and transport regimes on the deposition of hydrocarbons. The Great War Island is characterized by the influence of rivers Danube and Sava, channel Danube—Dunavac, as well as flooding in the inner part of the island. The shores of the Great War Island and the channel Veliki Galijaš are under constant sedimentation, while sedimentation in the channel Mali Galijaš occurs during major floods. The composition of sediments from the channel Veliki Galijaš and especially from the channel Mali Galijaš gives an insight of the condition over a longer period, while the coastal samples are constantly in contact with the high energy flow and their composition depends on the current river conditions.

The specific organic geochemical parameters indicate that most of the investigated samples mainly contain native organic matter with certain anthropogenic organic matter input. The n -alkane and diterpane patterns suggest the presence of immature organic matter of terrestrial origin. The native organic matter originates from higher land plants such as *Salix alba*, *Populus nigra*, *Fraxinus viridis*, *Taxodium distichum* Rich., various grass species, emergent, and submerged macrophytes such as *Salvinia natans*, *Nymphaea alba*, as well as from bacteria, algae, and phytoplankton. The Small War Island, a wetland environment, reflects specific sedimentation conditions characterized by the domination of diterpenes, pimarane, and phyllocladane in the saturated fraction.

The distributions of terpanes and steranes and the values of the corresponding maturity parameters, as well as the presence of unresolved complex mixture (UCM) indicate that the majority of investigated GWI sediments contain oil pollutants. Characteristic petroleum biomarkers and its derivatives have not been identified, or they are present in low abundance, in the central part of the Great War Island (channels Mali Galijaš and Veliki Galijaš). Coastal sediments of the Danube River are characterized by pronounced biodegradation of petroleum contaminants.

The presence of both native and mature organic matter unequivocally confirms the sedimentation of GWI's organic matter of autochthonous islands organic debris, as well as allochthonous organic matter brought by water, especially in coastal sediments.

Polycyclic aromatic hydrocarbons in the GWI's samples have a mixed origin, mostly from combustion and petroleum to a lesser extent. Domination of pyrogenic PAHs in GWI's samples implies that the incomplete combustion of organic matter is a dominant source of PAHs. The PAH ratios indicate a possible mixed combustion source, e.g., from petroleum, grass, wood, and/or coal combustion. Probably, they reach into sediments by atmospheric deposition and runoff from urban areas. Emissions of vehicles and boats are possible sources of petrogenic hydrocarbons. Deposition of PAHs from atmospheric sources is also continuingly occurring.

Acknowledgements The authors would like to thank the Ministry of Education, Science and Technological Development of Republic of Serbia (Grants Numbers: 451-03-9/2021-14/200026 and 451-03-9/2021-14/200168) for financial support. We are grateful to reviewers for useful comments and suggestions.

References

- Aloulou F, Kallel M, Dammak M, Elleuch B, Saliot A (2010) Even-numbered *n*-alkanes/*n*-alkenes predominance in surface sediments of Gabes Gulf in Tunisia. *Environ Earth Sci* 61:1–10
- Baumard P, Budzinski H, Garrigues P, Sorbe JC, Burgeot T, Bellocq J (1998) Concentration of PAHs (polycyclic aromatic hydrocarbons) in various marine organisms in relation to those in sediments and to trophic level. *Mar Pollut Bull* 30:951–960
- Bourbonniere RA, Meyers PA (1996) Sedimentary geolipid records of historical changes in the watersheds and productivities of Lakes Ontario and Erie. *Limnol Oceanogr* 41:352–359
- Budzinski H, Jones I, Bellocq J, Pierard C, Garrigues P (1997) Evaluation of sediment contamination by polycyclic aromatic hydrocarbons in the Gironde estuary. *Mar Chem* 58:85–97
- Das N, Chandran P (2011) Microbial degradation of petroleum hydrocarbon contaminants: an overview. *Biotechnol Res Int* 2011:941810
- Ficken KJ, Li B, Swain DL, Eglinton G (2000) An *n*-alkane proxy for the sedimentary input of submerged/floating freshwater aquatic macrophytes. *Org Geochem* 31:745–749
- Frysingher GS, Gaines RB, Xu L, Reddy CM (2003) Resolving the unresolved complex mixture in petroleum contaminated sediments. *Environ Sci Technol* 37:1653–1662
- Jovančičević B, Vrvic M, Schwarzbauer J, Wehner H, Scheeder G, Vitorović D (2007) Organic-geochemical differentiation of petroleum-type pollutants and study of their fate in Danube alluvial sediments and corresponding water (Pančevo oil refinery Serbia). *Water Air Soil Pollut* 183:225–238
- Kašanin-Grubin M, Štrbac S, Antonijević S, Djogo Mračević S, Randjelović D, Orlić J, Šajnović A (2019) Future environmental challenges of the urban protected area Great War Island (Belgrade Serbia) based on valuation of the pollution status and ecosystem services. *J Environ Manag* 251:109574
- Li Y, Yang S, Wang X, Hu J, Cui L, Huang X, Jiang W (2016) Leaf wax *n*-alkane distributions in Chinese loess since the Last Glacial Maximum and implications for paleoclimate. *Quat Int* 399:190–197
- Mackenzie AS (1984) Applications of biological biomarkers in petroleum geochemistry. In: Brooks J, Welte D (eds) *Advances in Petroleum Geochemistry*. Academic Press, London, pp 115–214
- Mille G, Asia L, Guiliano M, Malleret L, Doumenq P (2007) Hydrocarbons in coastal sediments from the Mediterranean Sea (Gulf of Fos area France). *Mar Pollut Bull* 54:566–575
- Off Gazette 50/93, 93/93, 10/94 (1994) Uredba o zaštiti prirodnih retkosti „Službeni Glasnik RS“. http://demo.paragraf.rs/demo/combined/Old/t/2009_06/t06_0386.htm (in Serbian). Accessed 15 Apr 2021.
- Off Gazette No7 (2005) Rešenje o stavljanju pod prirodnu zaštitu prirodnog dobra “Veliko Ratno ostrvo”, „Službeni Glasnik RS“ No 7. http://demo.paragraf.rs/demo/combined/Old/t/2005_04/t04_0168.htm (in Serbian). Accessed 15 Apr 2021.
- Otto A, Wilde V (2001) Sesqui- di- and triterpenoids as chemosystematic markers in extant conifers—a review. *Bot Rev* 67:141–238
- Peters KE, Walters C, Moldowan JM (2005) *The biomarker guide Biomarkers and isotopes in the environment and human history*, vol 1. University Press, Cambridge
- Ramdahl T (1983) Retene—a molecular marker of wood combustion in ambient air. *Nature* 306:580–582
- Samelak I, Balaban M, Antić M, Šolević Knudsen T, Jovančičević B (2020) Geochromatographic migration of oil pollution from a heating plant to river sediments. *Environ Chem Lett* 18:459–466
- Samelak I, Balaban M, Vidović N, Koljančić N, Antić M, Šolević Knudsen T, Jovančičević B, (2018) Application of alkane biological markers in the assessment of the origin of oil pollutants in the soil and recent river sediments (River Vrbas Bosnia and Herzegovina). *J Serb Chem Soc* 83:1167–1175
- Schwarzbauer J, Jovančičević B (2015) *Fundamentals in organic geochemistry—fossil matter in the geosphere*. Springer, Heidelberg
- Scheibye K, Weisser J, Borggaard OK, Larsen MM, Holm PE, Vammen K, Christensen JH (2014) Sediment baseline study of levels and sources of polycyclic aromatic hydrocarbons and heavy metals in Lake Nicaragua. *Chemosphere* 95:556–565
- Silva TR, Lopes SRP, Spörl G, Knoppers BA, Azevedo DA (2012) Source characterization using molecular distribution and stable carbon isotopic composition of *n*-alkanes in sediment cores from the tropical Mundaú-Manguaba estuarine-lagoon system Brazil. *Org Geochem* 53:25–33
- Soclo HH, Garrigues P, Ewald M (2000) Origin of polycyclic aromatic hydrocarbons (PAHs) in coastal marine sediments: case studies in Cotonou (Benin) and Aquitaine (France) areas. *Mar Pollut Bull* 40:387–396
- Stojadinović S, Jovančičević B, Šajnović A, Golumbeanu M, Almasan R, Dj J, BFickenrčeski I (2021) Organic-geochemical characteristics of the mud from the Techirghiol Lake Romania. *Fres Environ Bull* 02A:1595–1607
- Šijačić-Nikolić M, Vilotić D, Veselinović M, Mitrović S, Jokanović D (2010) Bald cypress (*Taxodiumdistichum* (L) rich) in the protected area “Veliko ratno ostrvo“. *Bull Facult for* 103:173–184

- Štrbac S, Gajica G, Šajnović A, Vasić N, Stojanović K, Jovančićević B (2014) The use of biological markers in the determination of the origin and type of organic matter in the sediments of the Tisza River. *J Serb Chem Soc* 79:597–612
- Tan Pei Jian B, Ul Mustafa MR, Hasnain Isa M, Yaqub A, Ho YCY (2020) Study of the water quality index and polycyclic aromatic hydrocarbon for a river receiving treated landfill leachate. *Water* 12:2877
- Tan YL, Heit M (1981) Biogenic and abiogenic polycyclic aromatic hydrocarbons in sediments from two remote Adirondack Lakes. *Geochim Cosmochim Acta* 45:2267–2279
- Varnosfaderany MN, Bakhtiari AR, Gu Z, Chu G (2014) Perylene as an indicator of land-based plant biomarkers in the southwest Caspian Sea. *Mar Pollut Bull* 80:124–131
- Volkman JK, Barrett SM, Blackburn SI, Mansour MP, Sikes EL, Gelin F (1998) Microalgal biomarkers: a review of recent research developments. *Org Geochem* 29:1163–1179
- Volkman JK, Holdsworth DG, Neill GP, Bavor HJ (1992) Identification of natural, anthropogenic and petroleum hydrocarbons in aquatic sediments. *Sci Total Environ* 112:203–219
- Wang C, Wang W, He S, Du J, Sun Z (2011) Sources and distribution of aliphatic and polycyclic aromatic hydrocarbons in Yellow River Delta Nature Reserve China. *Appl Geochem* 26:1330–1336
- Wang Z, Yang C, Yang Z, Brown CE, Hollebone BP, Stout SA (2016) Petroleum biomarker fingerprinting for oil spill characterization and source identification. In: Stout SA, Wang Z (eds) *Standard Handbook Oil Spill Environmental Forensics*, 2nd edn. Elsevier, Amsterdam
- Witt G, Trost E (1999) Polycyclic aromatic hydrocarbons in sediments of the Baltic Sea and the German coastal waters. *Chemosphere* 38:1603–1614
- Yang Z, Shah K, Fieldhouse B, Mirnaghi F, Hollebone BP, Lambert P, Goldthorp M, Brown CE, Yang C (2021) Characterization occurrence and natural attenuation of spilled light synthetic crude oil in a boreal freshwater ecosystem. *Fuel* 285:119276
- Yunker MB, MacDonald RW, Vingarzan R, Mitchell RH, Goyette D, Sylvestre S (2002) PAHs in the Fraser River basin: a critical appraisal of PAH ratios as indicators of PAH source and composition. *Org Geochem* 33:489–515

Publisher's Note Springer Nature remains neutral with regard to jurisdictional claims in published maps and institutional affiliations.

Authors and Affiliations

Sanja Stojadinović¹  · Aleksandra Šajnović¹ · Milica Kašanin-Grubin¹ · Gordana Gajica¹ · Gorica Veselinović¹ · Snežana Štrbac¹ · Branimir Jovančićević²

Aleksandra Šajnović
aleksandra.sajnovic@ihm.bg.ac.rs

Milica Kašanin-Grubin
milica.kasanin@ihm.bg.ac.rs

Gordana Gajica
gordana.gajica@ihm.bg.ac.rs

Gorica Veselinović
gorica.veselinovic@ihm.bg.ac.rs

Snežana Štrbac
snezana.strbac@ihm.bg.ac.rs

Branimir Jovančićević
bjovanci@chem.bg.ac.rs

¹ Department of Chemistry, University of Belgrade, Institute of Chemistry, Technology and Metallurgy, National Institute of the Republic of Serbia, Njegoševa 12, 11000 Belgrade, Serbia

² Faculty of Chemistry, University of Belgrade, Studentski trg 12-16, 11000 Belgrade, Serbia